



## Heat transfer by free convection from the inside surface of the vertical and inclined elliptic tube

K. Elshazly<sup>a</sup>, M. Moawed<sup>a,\*</sup>, E. Ibrahim<sup>b</sup>, M. Emara<sup>a,b</sup>

<sup>a</sup> *Department of Mechanical Engineering, Faculty of Engineering Shoubra, Zagazig University, 108 Shoubra Street, Shoubra 11689, Cairo, Egypt*

<sup>b</sup> *Faculty of Engineering, Zagazig University, Zagazig, Egypt*

Received 2 April 2004; accepted 18 July 2004

Available online 15 September 2004

---

### Abstract

Free convection from the inside surface of vertical and inclined elliptic tubes of axis ratio ( $a:b$ ) 2:1 with a uniformly heated surface (constant heat flux) is investigated experimentally. The effects of orientation angle ( $\alpha$ ) and inclination angle ( $\phi$ ) on the heat transfer coefficient were studied. The orientation angle ( $\alpha$ ) is varied from  $0^\circ$  (when the major axis is horizontal) to  $90^\circ$  (when the major axis is vertical) with steps of  $15^\circ$ . The inclination angle ( $\phi$ ) is measured from the horizontal and varied from  $15^\circ$  to  $75^\circ$  with steps of  $15^\circ$ . The vertical position is considered as a special case of the inclined case when  $\phi = 90^\circ$ . The experiments covered a range of Rayleigh number,  $Ra$  from  $2.6 \times 10^6$  to  $3.6 \times 10^7$ . The local and average Nusselt numbers are estimated for different orientation angles and inclination angles at different Rayleigh numbers. The results obtained showed that the local  $Nu$  increased with the increase of axial distance from the lower end of the elliptic tube until a maximum value near the upper end, and then, it gradually decreased. The average  $Nu$  increases with the increase of  $\alpha$  or  $\phi$  at the same  $Ra$ . The results obtained are correlated by dimensionless groups and with the available data of the inclined and vertical elliptic tubes.

© 2004 Elsevier Ltd. All rights reserved.

*Keywords:* Free convection; Constant heat flux; Elliptic tube; Angle of attack; Inclination angle

---

\* Corresponding author. Tel.: +20 124 209 009; fax: +20 247 527 50.  
E-mail address: [mmoawed@hotmail.com](mailto:mmoawed@hotmail.com) (M. Moawed).

## Nomenclature

$A$	the inner surface area of the electric tube, $\pi DL$
$a, b$	tube major and minor axis
$c$	specific heat of air at constant pressure
$D$	hydraulic diameter of the elliptic tube
$g$	gravity acceleration
$Gr$	Grashof number, $g\beta qD^4/k\nu^2$
$h$	local heat transfer coefficient, $q/(t_s - t_a)$
$h_m$	average heat transfer coefficient, $q/(t_{ms} - t_a)$
$k$	thermal conductivity
$L$	elliptic tube length
$Nu$	local Nusselt number, $hD/k$
$Nu_m$	average Nusselt number based on diameter, $h_mD/k$
$Pr$	Prandtl number, $c\mu/k$
$q$	heat flux, $W/(\pi DL)$
$R$	axis ratio of elliptic tube, $a/b$
$Ra$	Rayleigh number based on diameter, $Gr_D Pr$
$t_a$	ambient air temperature
$t_s$	inside wall temperature of the elliptic tube
$t_{ms}$	average inside wall temperature of the elliptic tube
$t_{mf}$	mean film temperature, $(t_{ms} + t_a)/2$
$W$	electric power of the main heater
$X$	axial distance measured from the elliptic tube entrance

### Greeks

$\alpha$	orientation angle (angle of attack)
$\phi$	inclination angle measured from horizontal axis
$\beta$	volumetric coefficient of thermal expansion
$\mu$	dynamic viscosity of air
$\nu$	kinematic viscosity of air, $\mu/\rho$
$\rho$	density of air

## 1. Introduction

The growing attention to free convection is related to its importance in several engineering applications. Free convection from cylinders or tubes of elliptic shapes have been receiving growing interest in the last few decades because of its employment in many practical fields in the area of energy conservation, design of solar collectors, heat exchangers, nuclear engineering, cooling of electrical and electronic equipments and many others.

Heat transfer studies of free convection from elliptic tubes are necessary for better thermal design of industrial applications. Tubes of elliptic cross-section have drawn special attention

since they were found to create less resistance to the cooling fluid, which results in less pumping power. Also, the elliptic tubes geometry is flexible enough to approach a circular tube when the axis ratio ( $R$ ) approaches unity and to approach a flat plate when the axis ratio ( $R$ ) tends toward zero.

It is useful to review the literature of circular tubes as a special case of the elliptic tubes. Free convective heat transfer from circular cylinders has been studied intensively in the past. Gageyama and Isumi [1] investigated natural convection inside a vertical tube numerically. They employed a finite difference technique to solve the boundary layer governing equations and obtained relations for the  $Nu_m$  against  $Gr Pr r/L$ . Davis and Perona [2] made a study of the development of free convection flow of a gas in a heated vertical open tube numerically and experimentally. The numerical investigation employed a finite difference method to solve the governing equations. A comparison between the numerical and experimental results was introduced. Ismael [3] conducted experimental work of natural convection from the inside surface of vertical cylinders to air. A correlation between  $Nu_m$  and  $Gr Pr$  was obtained in the range of  $Gr Pr$  from  $4.2 \times 10^7$  to  $1.02 \times 10^{10}$ . Abdul-Aziz [4] studied the heat transfer by natural convection from the inside surface of a uniformly heated tube at different angles of inclination. The experiments covered a range of  $Ra$  from  $1.44 \times 10^7$  to  $8.85 \times 10^8$ ,  $L/D$  from 10 to 31.4 and angle of inclination (measured from vertical position) from  $0^\circ$  to  $75^\circ$ . The results showed that the average  $Nu$  was a maximum when the tube was vertical. Sarhan et al. [5] presented an experimental study of natural convection inside open-ended horizontal and vertical annuli with different aspect ratios. Correlations of the dimensionless group of average  $Nu - Ra \times D/L$  were presented for the horizontal and vertical cases. The problem of natural convection inside horizontal and vertical annuli was studied by many investigators [6–9]. Khamis [7] and Al-Arabi et al. [8] conducted theoretical and experimental studies of natural convection heat transfer inside vertical annuli, the theoretical study for radius ratios of 0.26, 0.5 and 0.9 with two cases of heating the inner or outer tube while the other tube was adiabatic. Shehata [9] studied natural convection inside vertical, inclined and horizontal annuli of radius ratio of 0.73 with the inner tube heated and outer tube adiabatic.

However, study of free convection from elliptic tubes seems to have not received intensive attention compared with circular tubes, and most of the available studies were with free convection from the outside surface. Raithby and Hollands [10] studied the problem of natural convection from an elliptic cylinder with a vertical plate and a horizontal circular cylinder as special cases. The study was limited to the vertical major axis configuration. Merkin [11] studied the symmetrical case of the same problem of the elliptic cylinder when either the major axis or the minor axis was vertical. The study was based on the solution of the boundary layer equations, and results were obtained for the entire surface excluding the buoyant plume region. Hung and Mayinger [12] made an experimental study of natural convection from elliptic tubes with different orientations and with different axis ratios. A correlation of the average Nusselt number was reported. Badr and Shamsheer [13] solved the problem of free convection from an elliptic cylinder for Rayleigh numbers ranging from 10 to  $10^3$  and axis ratios ranging from 0.1 to 0.964. The solution covered the entire flow region with no boundary layer approximations. Badr [14] studied laminar natural convection from an isothermal elliptic tube with different orientations. The tube orientation varied from a horizontal to a vertical major axis, while the axis ratio varied from 0.4 to 0.98. The study revealed that the average Nusselt number is a maximum when the major axis is vertical. Elshazly et al. [15] conducted an experimental investigation of natural convection from

the inside surface of a horizontal elliptic tube. A correlation of average  $Nu$  as a function of  $Ra$  and rotation angle of the horizontal elliptic tube was obtained.

The above literature survey clearly indicates the lack of studies on free convection from the inside surface of elliptic tubes. Therefore, the objective of the present study is to provide experimental data on free convection heat transfer from open ended vertical and inclined elliptic tubes with a constant heat flux and with different orientation angles (angle of attack) and inclination angles.

## 2. Experimental apparatus and procedure

The experimental apparatus used in the present work is shown in Fig. 1. It consists of an elliptic tube (test section) mounted on a specially constructed frame. The frame has the capability of rotating the test section around its horizontal axis and changing its inclination angle. The rotation angle  $\alpha$  (angle of attack) can be read from a protractor mounted on the test section, and the inclination angle ( $\phi$ ) can be read from another protractor mounted on the frame. The elliptic tube is a copper one of 82 mm major axis, 41 mm minor axis with a thickness of 2 and 500 mm length. The outer surface of the elliptic tube is covered with an electric insulating tape on which nickel–chrome wire of 0.4 mm is uniformly wound to form the main heater as shown in Fig. 2. The main heater is covered with an asbestos layer of 55 mm thickness, on which another nickel–chrome wire of 0.4 mm is uniformly wound to form a guard heater. The guard heater is covered with a 40-mm thick asbestos layer. Two pairs of thermocouples are installed in the asbestos layer between the main heater and the guard heater. The thermocouples of each pair are fixed on the same radial line. The input to the guard heater is adjusted so that at steady state, the readings of the thermocouples of each pair become practically the same. Then, all the heat generated by the main heater is flowing inward to the elliptic tube.

Thirty two copper–constantan thermocouples of 0.4 mm diameter are soldered in slots milled in the axial and circumferential directions to measure the inner surface temperature of the elliptic tube. The thermocouples are distributed along eight generator lines ( $G_1$ – $G_8$ ) at equal circumferential distances on the surface of the elliptic tube and at seven stations at axial distances of 50, 120, 190, 250, 310, 390 and 450 mm from one end of the elliptic tube as shown in Fig. 3(a). Eight of the thermocouples are distributed on the circumference at the axial distances of 250 mm (middle of

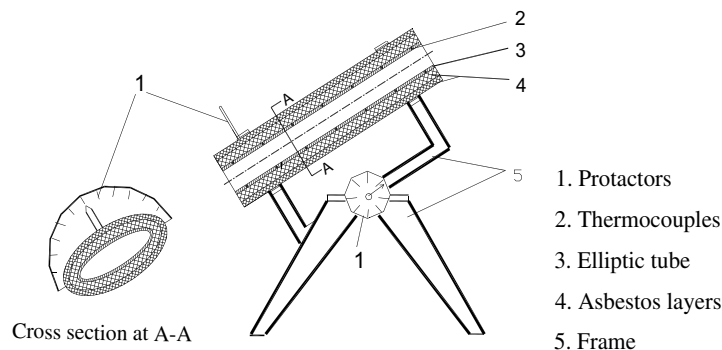


Fig. 1. Experimental setup.

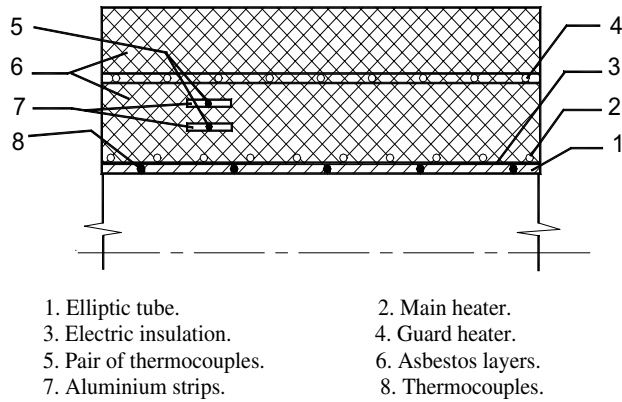


Fig. 2. Heaters arrangement.

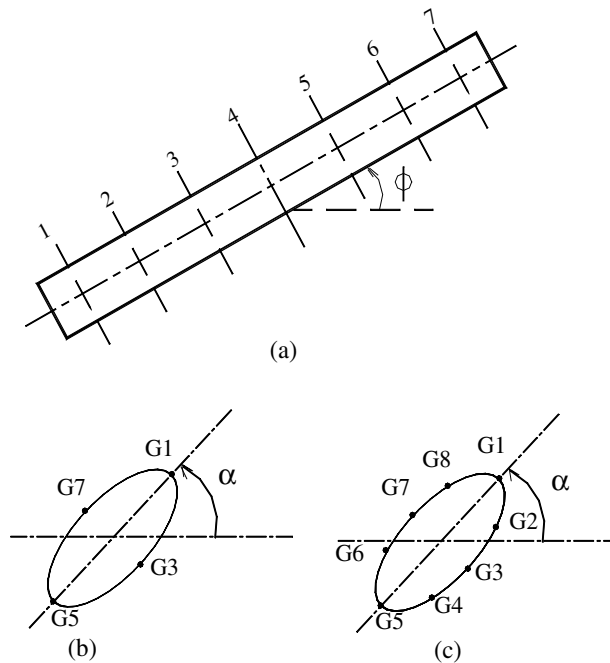


Fig. 3. Distribution of the thermocouples on the elliptic tube. (a) Thermocouples axial locations. (b) Axial location Nos. 1, 2, 3, 5, 6, 7. (c) Axial location No. 4.

elliptic tube), and four of the thermocouples are distributed on each of the other six stations of the elliptic tube as shown in Fig. 3(b).

The readings of all thermocouples are taken by means a precalibrated digital temperature recorder capable of reading 0.01 °C via a multi-switch. The ambient air temperature is measured by a precalibrated mercury in glass thermometer graduated in 0.1 °C intervals. The input electric power is regulated by an AC power variac and measured by a digital wattmeter with a resolution of 0.01 W.

The apparatus is mounted in a closed room 2.2 m × 2.2 m with plastic transparent walls to prevent currents of air, and the measuring instruments are mounted outside of this room. The input electric power to the main heater is controlled and changed by the AC variac at each experiment. The orientation angle is changed from zero to 90° with steps of 15°, and the inclination angle is changed from 15° to 90° with steps of 15°. The steady-state condition for each run is achieved after 3–4 h approximately. The steady-state condition is considered to be achieved when the temperature reading of each thermocouple did not change by more than 0.5 °C within 20 min. When the steady-state condition is established, the readings of all thermocouples, the input power and the ambient temperature are recorded.

### 3. Uncertainty analysis

Generally, the accuracy of experimental results depends upon the accuracy of the individual measuring instruments and the manufacturing accuracy of the elliptic tube. Also, the accuracy of an instrument is limited by its minimum division (its sensitivity). In the present work, the uncertainties in both heat transfer coefficient (Nusselt number) and Rayleigh number were estimated following the differential approximation method.

For a typical experiment, the total uncertainty in measuring the main heater input power, temperature difference ( $t_w - t_a$ ), heat transfer rate and the elliptic tube surface area were  $\pm 0.35\%$ ,  $\pm 0.46\%$ ,  $\pm 2.1\%$  and  $\pm 1.7\%$ , respectively. These were combined to give a maximum error of  $\pm 2.86\%$  in heat transfer coefficient (Nusselt number) and a maximum error of  $\pm 4.1\%$  in Rayleigh number.

### 4. Data reduction

In the present work, the local heat transfer coefficient between the inner surface of the elliptic tube and the air inside the elliptic tube is calculated from Eq. (1):

$$h = q / (t_s - t_a), \quad (1)$$

where  $q$  is the average heat flux transferred by free convection from the inside surface of the elliptic tube and is equal to the electric power. It was found that the heat transfer by radiation from the ends of the elliptic tube is less than 3% and can be neglected,

$$q = W / A. \quad (2)$$

The corresponding local Nusselt number  $Nu$  is calculated from:

$$Nu = h \times D / k. \quad (3)$$

The average heat transfer coefficient between the inner surface of the elliptic tube and the air inside the elliptic tube is calculated from Eq. (4):

$$h_m = q / (t_{ms} - t_a), \quad (4)$$

where

$$t_{ms} = \frac{1}{L} \int_0^L t_s dX. \tag{5}$$

The corresponding average Nusselt number,  $Nu$ , is calculated from Eq. (6):

$$Nu_m = h_m \times D/k. \tag{6}$$

The Rayleigh number,  $Ra$ , is calculated from:

$$Ra = Gr \times Pr. \tag{7}$$

The physical properties are evaluated at the mean film temperature, [16] as given by

$$t_{mf} = (t_{ms} + t_a)/2. \tag{8}$$

### 5. Results and discussion

Free convection of air is studied experimentally in vertical and inclined elliptic tubes of different orientation (rotation) and inclination angles. The inner surface of the elliptic tube is subjected to constant heat flux. The effects of orientation angle ( $\alpha$ ), inclination angle ( $\theta$ ) and  $Ra$  on the heat transfer results are discussed in this section. The results obtained in this work include the temperature distribution on the inner surface of the elliptic tube, local  $Nu$  and average  $Nu_m$ . The present experimental data covered ranges of  $Ra$  from  $2.6 \times 10^6$  to  $3.6 \times 10^7$ ,  $\alpha$  from  $0^\circ$  to  $90^\circ$  and  $\phi$  from  $15^\circ$  to  $75^\circ$  (inclined case) and  $\phi = 90^\circ$  (vertical case).

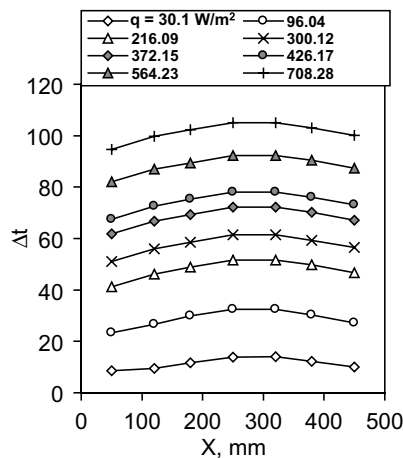


Fig. 4. Variation of  $\Delta t$  with  $X$  at  $\alpha = 0$  and  $\phi = 15$ .

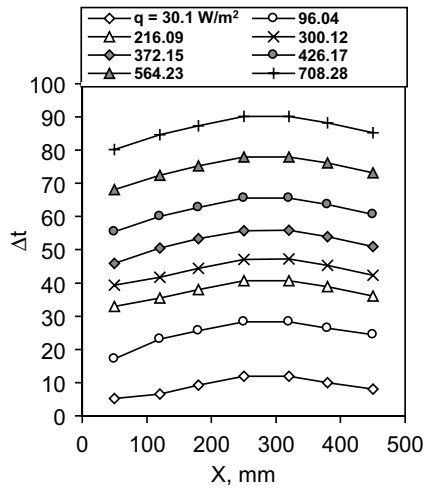


Fig. 5. Variation of  $\Delta t$  with  $X$  at  $\alpha = 0$  and  $\phi = 45$ .

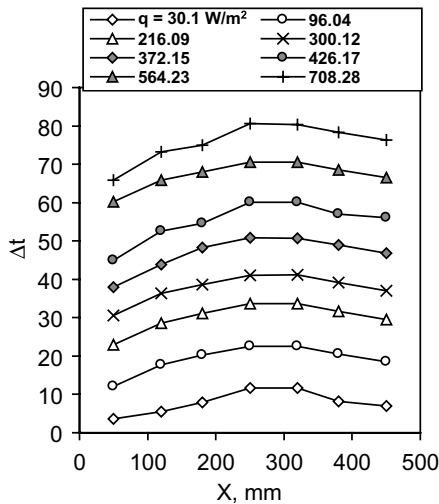


Fig. 6. Variation of  $\Delta t$  with  $X$  at  $\alpha = 0$  and  $\phi = 75$ .

*5.1. Temperature distribution*

Samples of the experimental temperature difference ( $\Delta t$ ) on the inner surface temperature of the elliptic tube are summarized in Figs. 4–10 for the inclined cases and in Fig. 11 for the vertical case for different heat fluxes and different  $\alpha$ s and  $\phi$ s. The temperature difference ( $\Delta t$ ) of all cases exhibits an increase in temperature gradient with increase of axial distance from the lower end until a maximum value occurs near the upper end, and then, it gradually decreases. The shapes of the  $\Delta t$ – $X$  curves agree well with the shapes of similar curves in the literature [1–4] of free



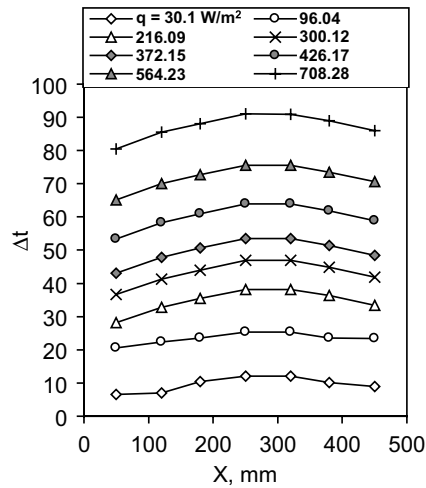


Fig. 7. Variation of  $\Delta t$  with  $X$  at  $\alpha = 90$  and  $\phi = 15$ .

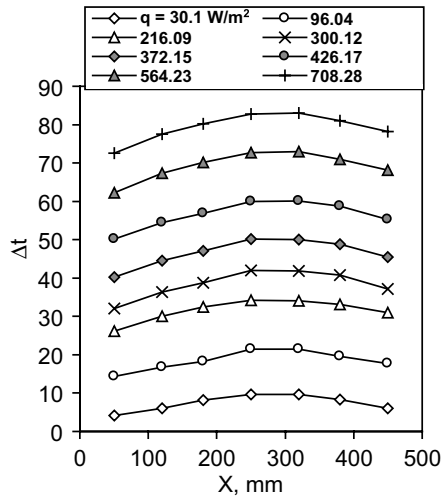


Fig. 8. Variation of  $\Delta t$  with  $X$  at  $\alpha = 90$  and  $\phi = 45$ .

convection inside circular tubes. This can be attributed to the flow of air entering from the lower end and flowing to the upper end due to the buoyancy effect. This flow causes a growth of the boundary layer from the lower end of the elliptic tube toward the upper portion where the increase of the turbulence intensity and the end effect cause a decrease in temperature. The effects of  $\phi$  and  $\alpha$  on the temperature difference ( $\Delta t$ ) are shown in Figs. 12 and 13, respectively. These figures show that the increase of  $\phi$  or  $\alpha$  reduce the temperature difference across the elliptic tube. The results of decreasing  $\Delta t$  with the increase of  $\phi$  is observed in [4] for free convection inside in-

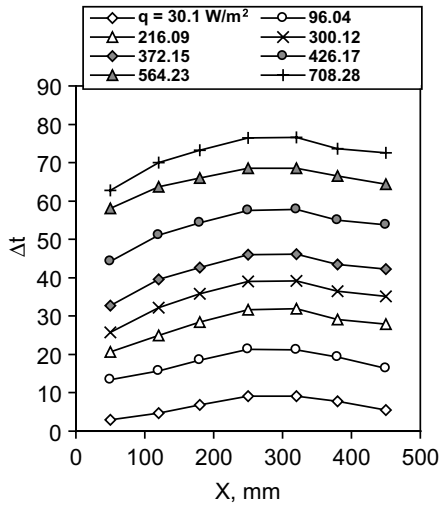


Fig. 9. Variation of  $\Delta t$  with  $X$  at  $\alpha = 90$  and  $\phi = 75$ .

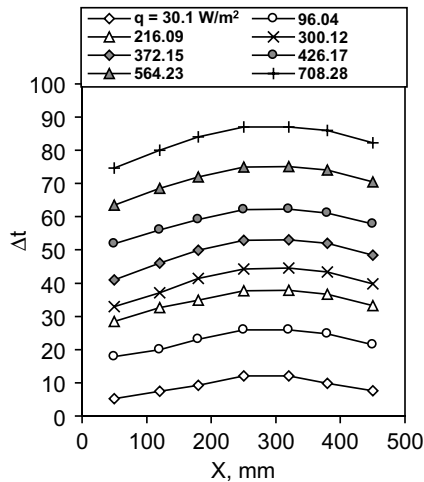


Fig. 10. Variation of  $\Delta t$  with  $X$  at  $\alpha = 45$  and  $\phi = 45$ .

clined circular tubes, and the results of decreasing  $\Delta t$  with the increase of  $\alpha$  is observed in [15] for free convection inside a horizontal elliptic tube.

It can be noticed that the circumferential variation of surface temperature measured at any axial location is small for any inclination and orientation of the test section. Generally, the maximum circumferential variation in temperature is  $\pm 1$  °C under constant heat flux conditions. This can be attributed to the high thermal conductivity of the elliptic tube and low Prandtl number of the air.

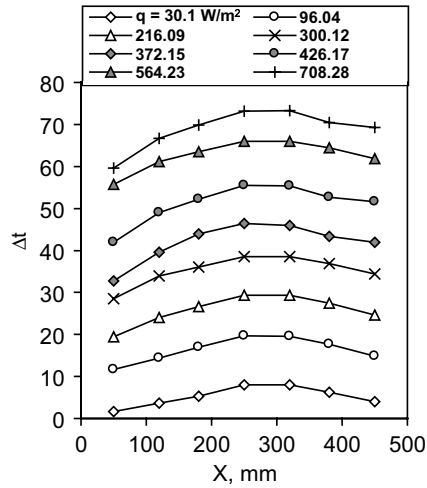


Fig. 11. Variation of  $\Delta t$  with  $X$  at  $\phi = 90$  (vertical case).

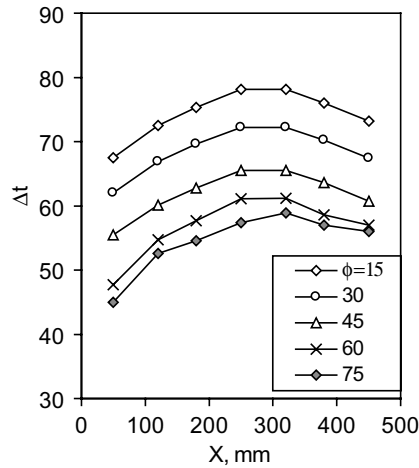


Fig. 12. Effect of  $\phi$  on  $\Delta t$  at  $\alpha = 0$  and  $q = 426.17$  W/m<sup>2</sup>.

### 5.2. Nusselt number

Figs. 14–20 show sample data of the local  $Nu$  vs.  $X/L$  for inclined cases at different heat fluxes and different  $\alpha$  and  $\phi$ . As shown in these figures, the local Nusselt number decreases with increase of axial distance from the lower end of the elliptic tube to a point near the upper end, and then, it gradually increases. This can be explained by noting that when the cold air is drawn from the lower end of the elliptic tube, it causes a higher heat transfer coefficient, and when the air coming up encounters the growing boundary layer, a decrease in heat transfer coefficient occurs. The increase

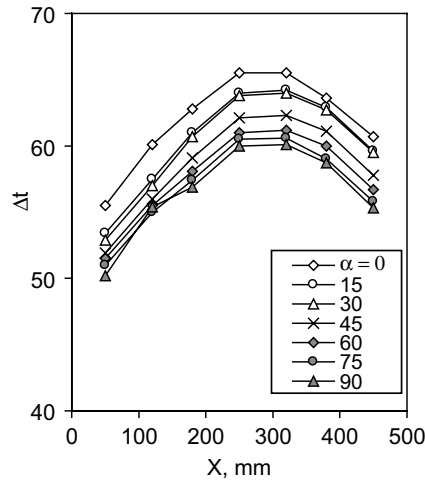


Fig. 13. Effect of  $\alpha$  on  $\Delta t$  at  $\phi = 45$  and  $q = 426.17 \text{ W/m}^2$ .

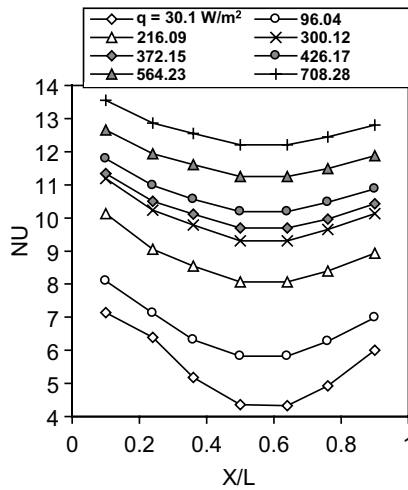


Fig. 14. Variation of  $Nu$  with  $X$  at  $\alpha = 0$  and  $\phi = 15$ .

of turbulence of the boundary layer at the upper portion of the elliptic tube and the end effect cause an increase in heat transfer coefficient near the upper end. Fig. 21 shows the variation of local Nusselt number  $Nu$  with axial distance for different heat fluxes and  $\phi = 90$  (vertical case). This figure shows that the  $Nu$  of the vertical case gives the same general shape as the inclined case, but it has greater values than the inclined case. This result also is observed in [4], which concluded that the heat transfer coefficient of a vertical circular tube gives a higher heat transfer than in an inclined case.

The effects of inclination angle  $\phi$  and orientation angle  $\alpha$  on  $Nu$  are shown in Figs. 22 and 23, respectively. These figures show that the  $Nu$  increases with the increase of  $\phi$  or  $\alpha$  with other

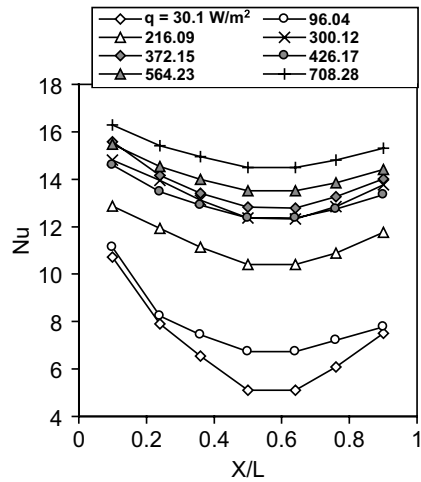


Fig. 15. Variation of  $Nu$  with  $X$  at  $\alpha = 0$  and  $\phi = 45$ .

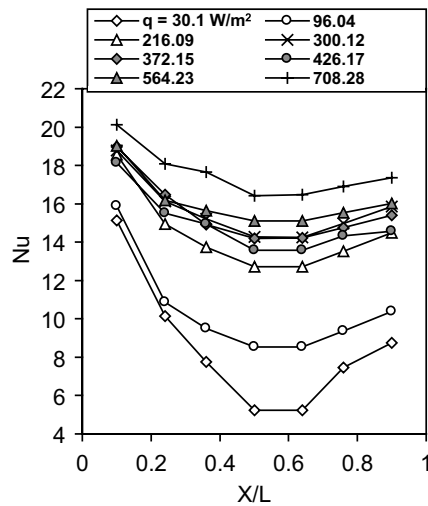


Fig. 16. Variation of  $Nu$  with  $X$  at  $\alpha = 0$  and  $\phi = 75$ .

conditions constant. The increasing of  $Nu$  with the increase of  $\phi$  can be attributed to the increase of boundary layer turbulence and the increased flow of air due the buoyancy force through the lower end of the elliptic tube. The increasing of  $Nu$  with the increase of  $\alpha$  is due to the increase of the quantity of air drawn on the inner hot surface of the elliptic tube. When  $\alpha = 0$ , it can be considered that there are approximately two flat surfaces (one facing upward and the other downward), and when  $\alpha$  increases, they tend to be two inclined surfaces until they become two vertical surfaces when  $\alpha = 90$ , which gives a higher heat transfer coefficient. This result agrees with the previous results of horizontal, inclined and vertical plates that showed that the heat transfer coefficient of a vertical plate is greater than that of an inclined

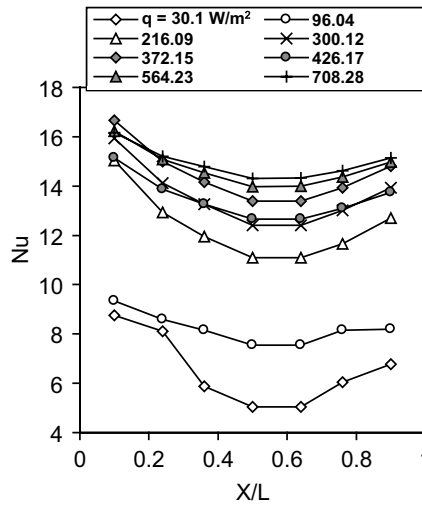


Fig. 17. Variation of  $Nu$  with  $X$  at  $\alpha = 90$  and  $\phi = 15$ .

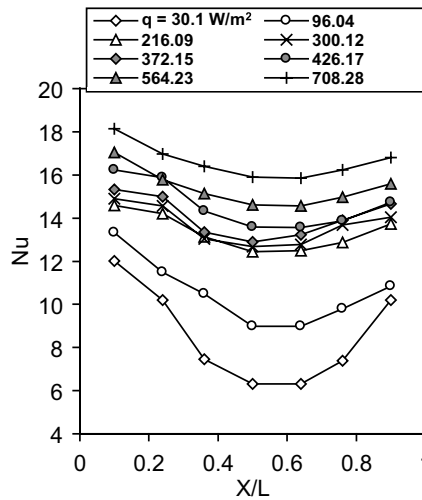


Fig. 18. Variation of  $Nu$  with  $X$  at  $\alpha = 90$  and  $\phi = 45$ .

plate facing up or down and, in turn, is greater than that of a horizontal plate facing up or down.

The variation of the average Nusselt number  $Nu_m$  vs.  $Ra$  for inclined and vertical elliptic tubes is shown in Figs. 24–27. The effect of  $\phi$  on  $Nu_m$  is shown in Figs. 24 and 25 for  $\alpha = 0$  and  $90$ , respectively, and the effect of  $\alpha$  on  $Nu_m$  is shown in Fig. 26. The effects of  $\phi$  and  $\alpha$  on  $Nu_m$  are similar to the effects on local  $Nu$  explained before.  $Nu_m$  increases with the increase of  $\phi$  or  $\alpha$  at the same  $Ra$ . The variation of  $Nu_m$  vs.  $Ra$  for  $\phi = 90$  (vertical case) is shown in Fig. 27. With the fact that there is no effect of  $\alpha$  on  $Nu_m$  in the vertical case, it gives greater values of  $Nu_m$  than all cases of the inclined elliptic tube.

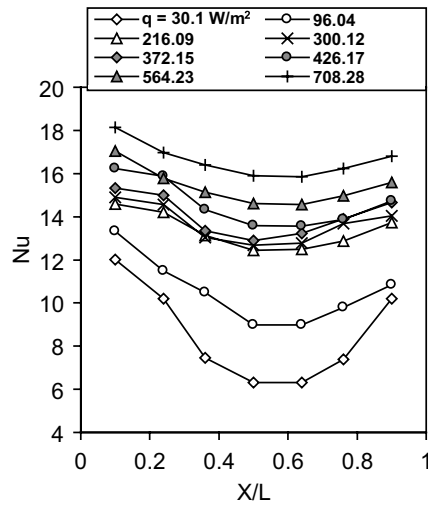


Fig. 19. Variation of  $Nu$  with  $X$  at  $\alpha = 90$  and  $\phi = 75$ .

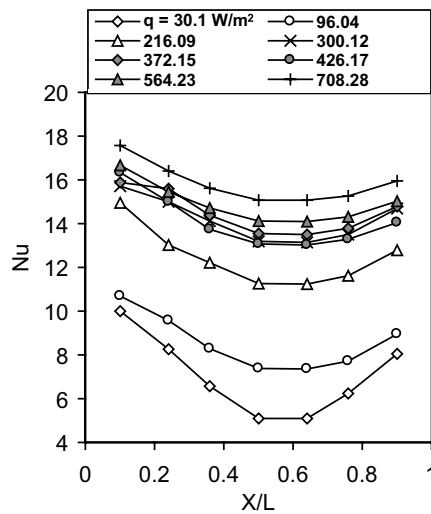


Fig. 20. Variation of  $Nu$  with  $X$  at  $\alpha = 45$  and  $\phi = 45$ .

### 5.3. Correlation of the results

The general correlation of  $Nu_m$  as a function of  $Ra$ ,  $\sin \alpha$  and  $\sin \phi$  for the inclined elliptic tube is given by

$$Nu_m = C_1 Ra^n \sin^m \alpha \sin^k \phi, \tag{9}$$

and that for  $Nu_m$  as a function of  $Ra$  only for a vertical elliptic tube is given by

$$Nu_m = C_2 Ra^q, \tag{10}$$

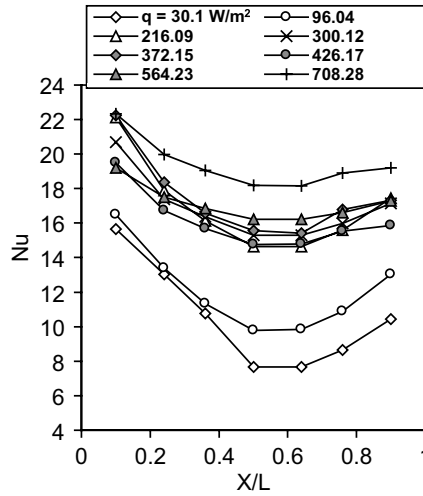


Fig. 21. Variation of  $Nu$  with  $X$  at  $\phi = 90$  (vertical case).

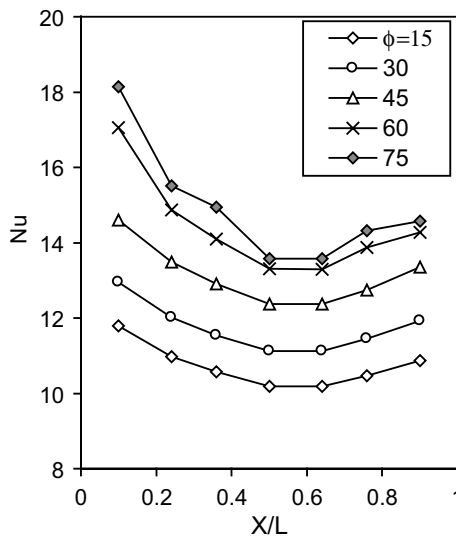


Fig. 22. Effect of  $\phi$  on  $Nu$  at  $\alpha = 0$  and  $q = 426.17 \text{ W/m}^2$ .

where  $C_1, n, m, k, C_2$  and  $q$  are constants.

The experimental results are fitted, using power regression, to determine the constants. The resulting empirical correlations are:

- For the inclined elliptic tubes:

$$Nu_m = 0.102Ra^{0.308} \sin^{0.022} \alpha \sin^{0.194} \phi, \quad 2.6 \times 10^6 < Ra < 3.5 \times 10^7; \quad 0 < \alpha < 90 \text{ and } 15 < \phi < 75. \tag{11}$$



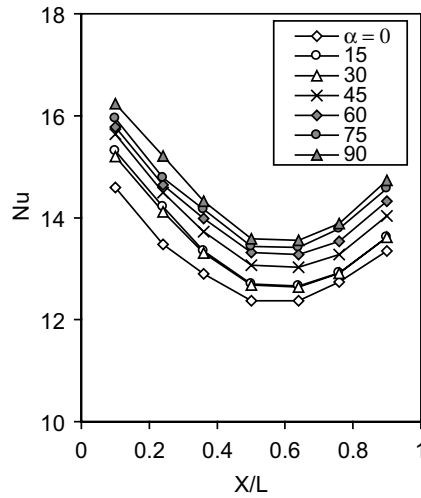


Fig. 23. Effect of  $\alpha$  on  $Nu$  at  $\phi = 45$  and  $q = 426.17 \text{ W/m}^2$ .

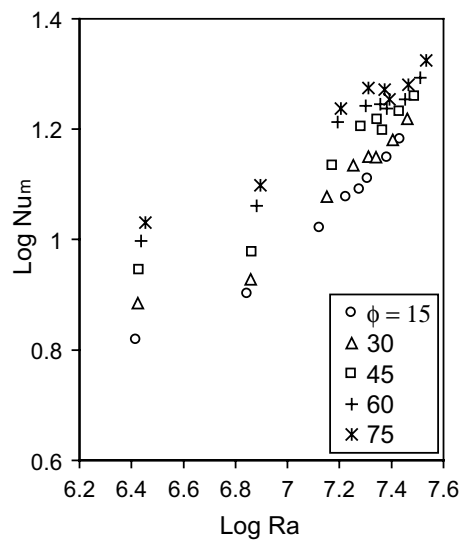


Fig. 24. Average  $Nu$  vs.  $Ra$  for  $\alpha = 0$ .

The calculated data from Eq. (11) of the average Nusselt number  $Nu_{mCal}$  is plotted against experimental data of the average Nusselt number  $Nu_{mExp}$  in Fig. 28. As shown in this figure, the maximum deviation between the experimental data and the correlation for the inclined elliptic tube is  $\pm 20\%$ .

- For the vertical elliptic tube:

$$Nu_m = 0.165Ra^{0.284}, \quad 2.8 \times 10^6 < Ra < 3.6 \times 10^7. \tag{12}$$

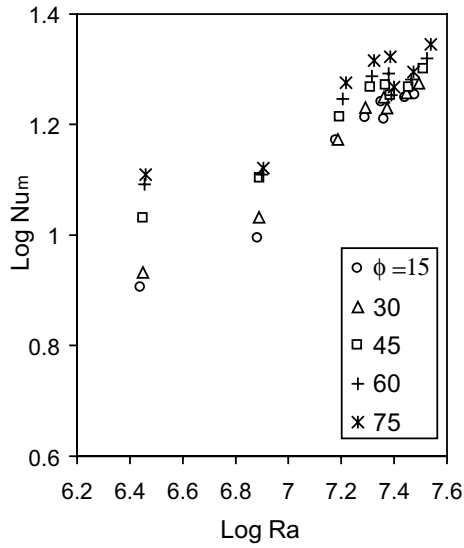


Fig. 25. Average  $Nu$  vs.  $Ra$  for  $\alpha = 90$ .

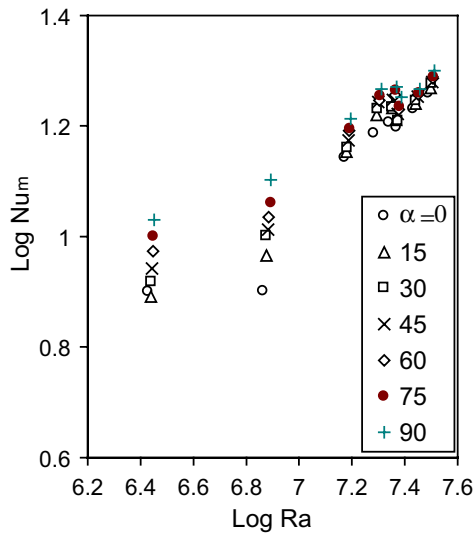


Fig. 26. Average  $Nu$  vs.  $Ra$  for  $\phi = 45$ .

Eq. (12) represents the general equation for free convection inside vertical elliptic tubes.

The experimental results are compared with Eq. (12) in Fig. 29. As can be seen from this figure, Eq. (12) represents the experimental results with a maximum deviation of  $\pm 9\%$ .

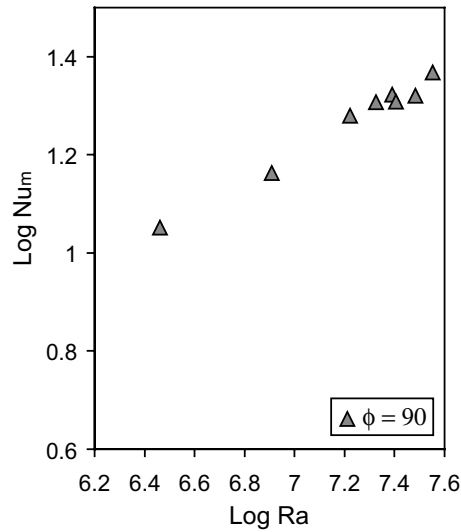


Fig. 27. Average  $Nu$  vs.  $Ra$  for  $\phi = 90$  (vertical case).

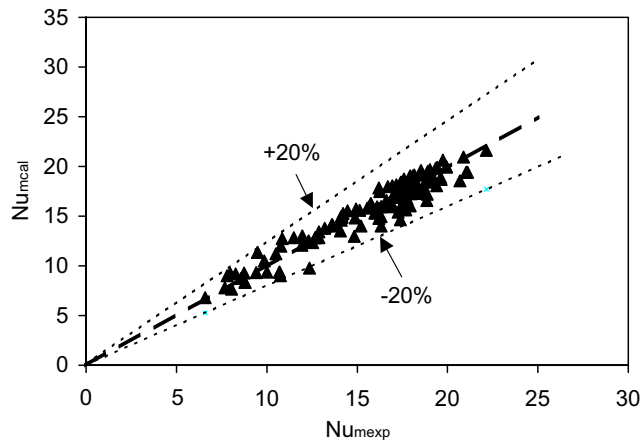


Fig. 28.  $Nu_{mcal}$  against  $Nu_{mexp}$  for inclined elliptic tube.

### 6. Comparison with previous work

As mentioned in the literature review, there is no available information about free convection heat transfer inside inclined and vertical elliptic tubes, so the available information about free convection from inclined circular tubes by Abdul-Aziz [4] is used for comparison. The present experimental data for inclined elliptic tubes at  $\phi = 45$  and  $\alpha = 0$  is recalculated in the same way as Abdul-Aziz [4] to compare with the inclined circular tube at  $\phi = 45$  as shown in Fig. 30. This figure shows that the present results of free convection inside inclined elliptic tubes are higher than the results of Abdul-Aziz [4] for free convection inside inclined circular tubes. This comparison

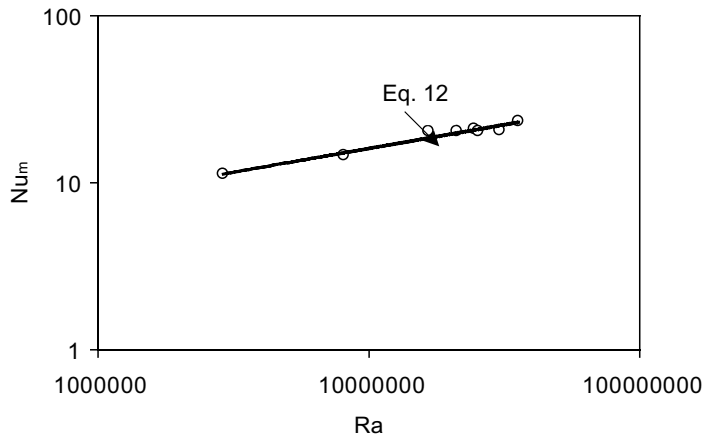


Fig. 29. Comparison of experimental data of vertical elliptic tube with Eq. (12).

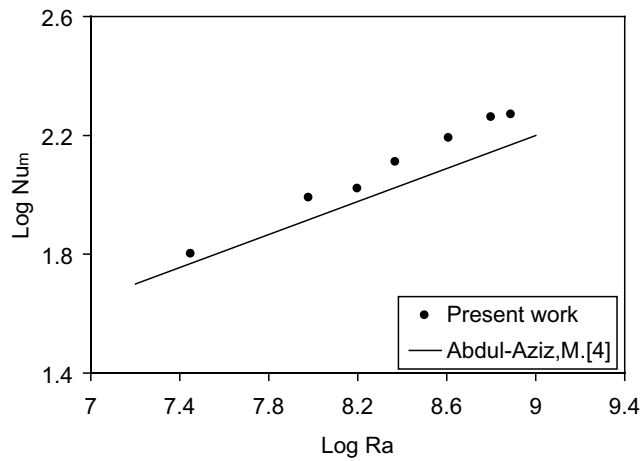


Fig. 30. Comparison between present work and Abdul-Aziz [4] at  $\phi = 45^\circ$ .

gives an important result, namely, that the heat transfer coefficient from the inside surface of an elliptic tube at any angle of rotation is higher than that from the inside of a circular tube. In general, there is a good enhancement of the free convection heat transfer by using an elliptic tube at any rotation and inclination angle instead of a circular tube at the same working conditions.

### 7. Conclusion

Free convection heat transfer from the inside surface of inclined and vertical elliptic tubes of axis ratio 2:1 with a uniformly heated surface is investigated experimentally. The orientation angle  $\alpha$  is changed from  $0^\circ$  to  $90^\circ$  with steps of  $15^\circ$ , and the inclination angle  $\phi$  is changed from  $15^\circ$  to

75° with steps of 15° (inclined case). The inclination angle  $\phi = 90^\circ$  (vertical case) is considered a special case of the inclined case and is studied separately. The experiments covered a range of Rayleigh number  $Ra$  from  $2.6 \times 10^6$  to  $3.6 \times 10^7$ . The local and average heat transfer coefficients and Nusselt number are estimated for different orientation angles  $\alpha$  and inclination angles  $\phi$  at different Rayleigh numbers. It is found that the temperature distributions and the local  $Nu$  increase with the increase of axial distance from the lower end of the elliptic tube until a maximum value is reached near the upper end, and then, they gradually decreased. Also, they increase with the increase of  $\alpha$  at the same axial distance. The average  $Nu$  increases with the increase of  $\alpha$  or  $\phi$ . Correlations of Nusselt number for free convection inside inclined elliptic tubes at different orientation angles and inclination angles and for vertical elliptic tubes are presented.

## References

- [1] Gageyama M, Isumi R. Bull JSME 1970;13:282–394.
- [2] Davies P, Perona J. Int J Heat Mass Transfer 1971;14:889–903.
- [3] Ismaeel KA. M.Sc. Thesis, University of Technology, Baghdad, Iraq; 1977.
- [4] Abdul-Aziz M. Ms. Thesis, Mechanical Engineering Department, Al-Azhar University, Cairo, Egypt; 1991.
- [5] Sarhan A, Kamis M, Moawed M. Al-Azhar Univ Eng J 2001;4(4):327–41.
- [6] El-Shaarawi MA, Sarhan A. Int Eng Chem Fundam 1981;20:388–94.
- [7] Khamis M. Ph.D. Thesis, Mechanical Engineering Department, Al-Azhar University, Cairo, Egypt; 1982.
- [8] Al-Arabi MA, El-Shaarawi MAI, Khamis M. Int J Heat Mass Transfer 1987;30:1381–9.
- [9] Shehata A. M.Sc. Thesis, Al-Azhar University, Cairo, Egypt; 1989.
- [10] Raithby GD, Hollands KG. ASME J Heat Transfer 1976;98:72–80.
- [11] Merkin JH. ASME J Heat Transfer 1977;99:453–7.
- [12] Hung SY, Mayinger F. Warme Stoffubertrag 1984;18:175–83.
- [13] Badr HM, Shamsheer K. Int J Heat Mass Transfer 1993;36:1457–64.
- [14] Badr HM. ASME J Heat Transfer 1997;119:709–18.
- [15] El-Shazly K, Moawed M, Ibrahim E, Emara M. Cairo international conference on energy and environment; January 4–7 2003.
- [16] Kays WM, London AL. Technical Report 23, Stanford University; 1954.